

Propane Oxidative Dehydrogenation on $\text{BiP}_{1-x}\text{V}_x\text{O}_4$ Supported Titania Catalysts

Mbarka Ouchabi^a, Ilyasse Loulidi^{*b}, Mahfoud Agunaou^a

a) Laboratory of Catalysis and Corrosion of Materials, Chouaib Doukkali University, Faculty of Sciences El Jadida, BP. 20, El Jadida, Morocco

b) Laboratory of Chemistry and Biology Applied to the Environment, Faculty of Sciences, Moulay Ismail University, BP 11201-Zitoune, Meknes, Morocco

Received 30 October 2022; revised form 21 November 2022; accepted 18 December 2022 (DOI: 10.30495/IJC.2022.1971843.1970)

ABSTRACT

The molecularly dispersed $\text{BiP}_{1-x}\text{V}_x\text{O}_4/\text{TiO}_2$ supported materials, with x varying from 0 to 1, were prepared by impregnation of Bismuth, Phosphorus, and Vanadium on a Titanium Oxide TiO_2 support. Their structures were characterized by different techniques including X-ray diffraction, Spectroscopic Raman, temperature-programmed reduction of the catalysts in H_2 (H_2 -TPR), and by the methanol oxidation reaction. This very sensitive technique provided us with relevant information on the nature of the catalytic active sites (acid-base and redox) of the phases dispersed on the support. The characterization results show the structural evolution of $\text{BiP}_{1-x}\text{V}_x\text{O}_4$ species, from isolated BiPO_4 crystallites for $x = 0$, to BiVO_4 crystallites $x = 1$. The oxidation of methanol showed the acidic properties of the $\text{BiPO}_4/\text{TiO}_2$ catalyst, through the formation of dimethyl ether as the major product of the reaction. The substitution of phosphorus by vanadium promotes the formation of formaldehyde, confirming the presence of redox sites. These catalysts were examined in the oxidative dehydrogenation (ODH) of propane to propene. For $x > 0.5$, dispersed BiVO_4 exhibited higher levels of propane ODH than BiPO_4 crystallites, consistent with their greater reducibility probed by temperature-programmed reduction of H_2 and the presence of redox sites confirmed by methanol oxidation, with good selectivity to propene. Catalysts with $x = 0$, were less selective to propene due to favorable propylene combustion during its formation. A thorough understanding of the intrinsic catalytic properties of the $\text{BiP}_{1-x}\text{V}_x\text{O}_4/\text{TiO}_2$ oxides and in particular the BiPO_4 and BiVO_4 crystallites provides relevant information on the structural requirements of the propane ODH reaction, of interest for the design of more efficient Bi-P-V-O based catalysts for propene production. The results show that all substituted catalysts exhibit significant propene selectivity. In addition, the $\text{BiP}_{0.7}\text{V}_{0.3}\text{O}_4/\text{TiO}_2$ catalyst exhibits high activity with good propene selectivity. This catalytic activity was correlated with high reducibility.

Keywords: $\text{BiP}_{1-x}\text{V}_x\text{O}_4/\text{TiO}_2$ catalyst; methanol oxidation; Propane oxidative dehydrogenation.

1. Introduction

Much research has been devoted to the activation and functionalization of alkanes, particularly in the area of heterogeneous catalysis of molecular oxygen oxidation. For example, the oxidative dehydrogenation of alkanes to alkenes [1–6] has been widely studied for its attractive economic potential as an alternative route to alkenes. Oxidative Dehydrogenation of propane (ODHP) has the advantage of being an exothermic reaction, thermodynamically favorable, operating at lower temperatures, and less prone to catalyst deactivation by coking than the dehydrogenation reaction.

The scientific obstacle is the high reactivity of propene in the presence of oxygen compared to propane, and thus the difficulty of activating propane at moderate temperatures while avoiding over-oxidation to CO_x . Performance improvement [7].

However, to be competitive, ODHP requires a substantial improvement of the catalyst performance. The latter relies on the understanding of their mode of operation and the consideration of structural parameters that can ensure the crucial steps of the reaction mechanism. A good ODHP catalyst is more than a bifunctional system and requires more than the simple combination of acid-base and redox properties. Indeed, given the particular mode of operation of soft oxidation,

www.SID.ir

*Corresponding author:

E-mail address: il.loulidi@gmail.com (I. Loulidi)

Archive of SID

catalysts that is inherent to the specifics of the Mars and Van Krevelen mechanism, the reaction is sensitive to the structure of the material [8].

Recently, promising results have been reported for bulk and supported vanadium-phosphorus catalysts [9–12]. Vanadium-phosphorus (VPO) mixed materials have been known as hydrocarbon conversion catalysts since their industrial use in the conversion of n-butane to maleic anhydride [13–15]. The particular aspect of these catalysts results from the in situ formation at a temperature of the active phase from the hydrated precursors [15].

In addition, the use of supported OPV catalysts is normally more attractive for a larger surface-to-volume ratio of the active components and for better heat transfer. The distribution of the oxide on the quasi-inert matrix leads to the formation of centers with specific chemical and physical characteristics and reactivity. Several common metal oxides such as TiO₂, SiO₂, MgO, and Al₂O₃ have been used as supports for V and VPO catalysts in alkane ODH [13–17]. Other vanadium MVO (M = Mg, Sb, Mo) containing systems [18–20] have shown more promising catalytic performance in alkane ODH when supported on the usual metal oxides.

Vanadium phosphate supported on the surface of porous materials offers the possibility of combining the unique textural and acid-base properties of the support materials with the redox properties of the V-P oxide species, which opens the possibility of activating alkanes at relatively low temperatures.

Previous studies on the ODH reaction of propane carried out on supported vanadium catalysts revealed that vanadium supported on TiO₂ is more active than when supported on ZrO₂, Al₂O₃, and MgO [21]. Similarly, TiO₂ as a support seems to be more interesting and promising for better dispersion of the active phase of VPOs (Vanadium-Phosphorus Oxide) [22].

Our objective in this study is to explore the influence of vanadium incorporation in the BiPO₄/TiO₂ system, in terms of textural and structural properties and then on the catalytic performance in propane ODH. The catalyst synthesized by the wet impregnation technique is first characterized by X-ray diffraction. In addition, we used temperature-programmed reduction (TPR) to study the influence of redox properties on catalytic activity and mild methanol oxidation as a catalytic surface probe to investigate the surface properties of titanium-supported BiP_{1-x}V_xO₄ samples [23].

2. Experimental

2.1. Catalysts preparation

A series of BiP_{1-x}V_xO₄/TiO₂ catalysts were prepared using a Titanium oxide support[8] and with a P/V mole fraction of 9/1, 8/2, 7/3, 6/4, 5/5, 4/6, 3/7, 2/8 and 1/9 (x = 0, 0.1, 0.2, 0.3, 0.4, 0.5, 0.6, 0.7, 0.8, 0.9, 1). The titanium oxide used is of the type: anatase whose specific surface is 7.15 m²/g. These catalysts were prepared by the successive wet impregnation technique using a solution of Bi(NO₃)₃.5H₂O, NH₄VO₃, and H₃PO₄. According to the following mechanism, a mass of 91.1 g of bismuth nitrate Bi(NO₃)₃.5H₂O was dissolved in 50 mL of distilled water containing 2.5N HNO₃ under magnetic stirring to produce a homogeneous solution and then impregnated onto a well-defined quantity of titanium oxide (15 g). The impregnated Bi/TiO₂ catalysts were dried for 12 hours at a temperature of 393K and then calcined under a stream of air at 673 K for 4 hours. A second impregnation on Bi/TiO₂ was performed using an aqueous solution of NH₄VO₃ and H₃PO₄. Then, the impregnated catalysts were dried again for 12 h at 393K, then calcined under a stream of air at 673 K for 4 h.

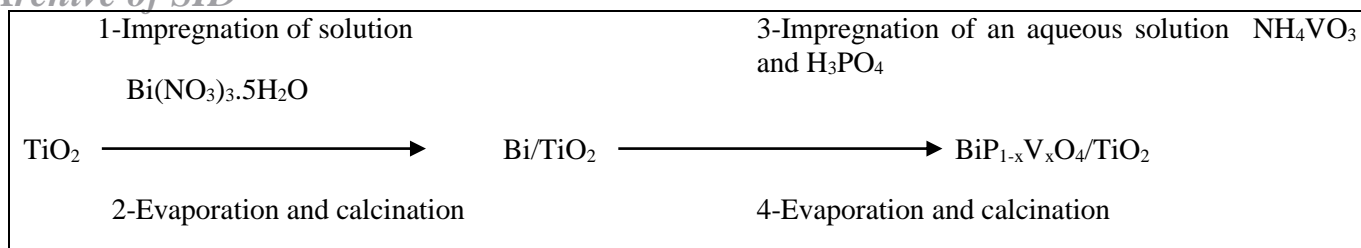
2.2. Characterization

X-ray diffraction: (XRD) was carried out using a Siemens (D500) diffractometer and monochromatic CuK α ($\lambda = 1.5406 \text{ \AA}$). Scans were obtained in the 2θ range 10° to 70°, with a step size of 0.04° every 2s.

Spectroscopic Raman: Raman spectra were recorded at room temperature on a Perkin Elmer system 2000R, equipped with an Nd: Yag near IR laser, Neodymium doped with yttrium-aluminum producing radiation at 1064 nm. The detector is Ga As. The control of the spectrophotometer and the data acquisition are done with a microcomputer. The frequencies are assigned using data from the literature.

The BET surface areas were determined by N₂ physisorption at 77 K using a Flow Sorb 2300 analyzer. A known amount of catalyst is degassed with a 30% N₂ / 70% He, mixture at 300 °C for 1/2 hour. This technique consists in determining the quantity adsorbed equivalent to a monolayer of probe molecule (N₂) on the solid to be studied. The surface of the monolayer being equal to the surface of the solid, it suffices to determine the amount equivalent to a monolayer of adsorbed nitrogen to obtain the specific surface of the solid.

The TPR profiles were obtained by injecting an H₂/Ar through the sample (about 70 mg). The temperature was increased from 25 °C to 900 °C at a rate of 5 °C/min, and the amount of H₂ consumed was determined with a thermo-conductivity detector.



Methanol oxidation was studied by the flow method. The composition of the reactant feed $\text{CH}_3\text{OH}/\text{O}_2/\text{H}_2$ was in a molar ratio of 7.1/15.5/77.4, corresponding to a partial pressure of 54 torrs. The reactant mixture was obtained by passing an O_2/He mixture through a methanol saturator maintained at 10 °C. The overall flow rate and the amount of catalyst were adjusted in order to secure a moderate methanol conversion not exceeding 10%. The reaction rates are expressed as the methanol consumption for the formation of a given product. The reaction temperature was fixed at 250 °C.

Catalyst testing: The catalytic measurements in the ODH reaction were performed at atmospheric pressure on the temperature at 480 °C, by a conventional continuous flow quartz reactor. The molar composition of the reaction mixture was $\text{C}_3\text{H}_8/\text{O}_2/\text{He} = 10/10/80$ (mol %). All the tests were carried out using 1g of catalyst sample.

3. Results and Discussion

3.1. Structural characterization

3.1.1. X-ray diffraction

The XRD diagrams of $\text{BiP}_{1-x}\text{V}_x\text{O}_4/\text{TiO}_2$ catalysts with different V contents ($0 \leq x \leq 1$) are presented in **Fig. 1** and **Table 1**. For $x = 0$, $x = 0.3$, and $x = 0.5$, the XRD shows small lines characteristic of the monazite phase (reference code 00-001-0812). Above $x = 0.5$, the XRD diagrams show the presence of vanadium oxides V_3O_7

(24°) (reference code 01-071-0454), in addition to the fergusonite phase BiVO_4 (18°, 28°, 31°) (reference code 01-075-2480).

In comparison with our previous study carried out on unsupported $\text{BiP}_{1-x}\text{V}_x\text{O}_4$ catalysts (**Figs 2 and 3**), the weak lines of the BiPO_4 crystallites for $x \geq 0.5$ may be due to the good dispersion of the latter on the titanium support (**Fig. 2**). On the other hand, for $x > 0.5$, the lines corresponding to BiVO_4 crystallites are well shown.

3.1.2. Spectroscopic Raman

Fig. 4, shows the Raman spectra of the Bi/TiO_2 -(P+V) catalysts. We can note the bands located at 160, 200, 400, 510, and 650 cm^{-1} . These characterize the presence of the TiO_2 anatase phase [27]. It can be seen that only the bands of the bare support are visible.

However, it should be noted that the intensity of the Raman signal decreases when the vanadium content increases, which could indicate that the covering of the support by crystallites of the $\text{BiP}_{1-x}\text{V}_x\text{O}_4$ phase increases with x , in other words, the dispersion decreases with the vanadium content

These results are consistent with the XRD spectra (**Fig. 4**), where it can be seen that only the bare support bands are visible for $x < 1$. As the vanadium content increases, the Raman signal intensity decreases, confirming the XRD results, and the support is well covered by the crystallites of the BiVO_4 phase, indicating a low dispersion of BiVO_4 crystallites in these catalysts.

Table 1. The different phases identified by XRD of prepared catalysts.

Initial conditions: All catalysts are calcined at 650 °C. The 2θ were scanned from 10 to 70 °.

x	Sample	Identified phases	Reference code	reference code
0	$\text{BiPO}_4/\text{TiO}_2$	BiPO_4 (Monazite)	00-001-0812	
0.3	$\text{BiP}_{0.7}\text{V}_{0.3}\text{O}_4/\text{TiO}_2$	BiPO_4 (Monazite)	00-001-0812	
0.5	$\text{BiP}_{0.5}\text{V}_{0.5}\text{O}_4/\text{TiO}_2$	BiPO_4 Monazite	00-001-0812	
		BiVO_4 (Fergusonite)	01-075-2480	
0.7	$\text{BiP}_{0.3}\text{V}_{0.7}\text{O}_4/\text{TiO}_2$	BiVO_4 (Fergusonite)	Refer	01-075-2480
1	$\text{BiVO}_4/\text{TiO}_2$	BiVO_4 (Fergusonite)	01-075-2480	
		V_3O_7	01-071-0454	

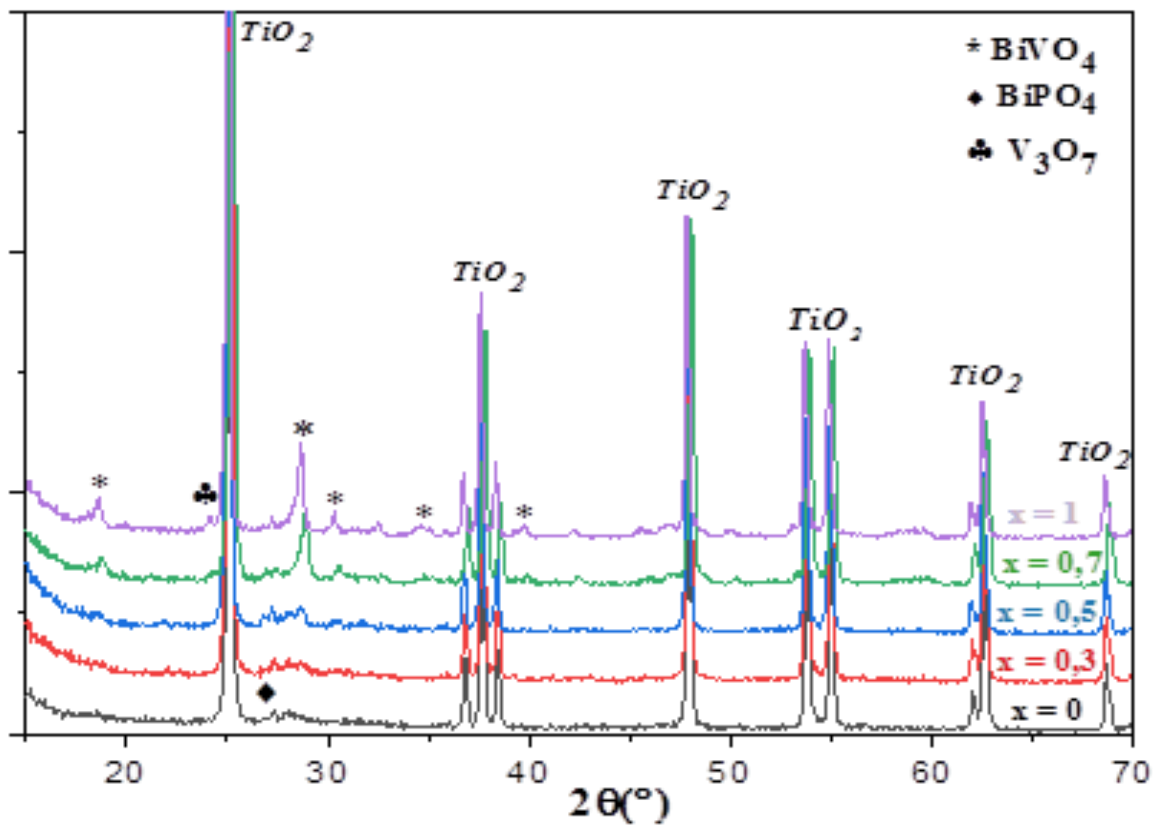


Fig. 1. XRD patterns of $\text{BiP}_{1-x}\text{V}_x\text{O}_4/\text{TiO}_2$ catalysts.

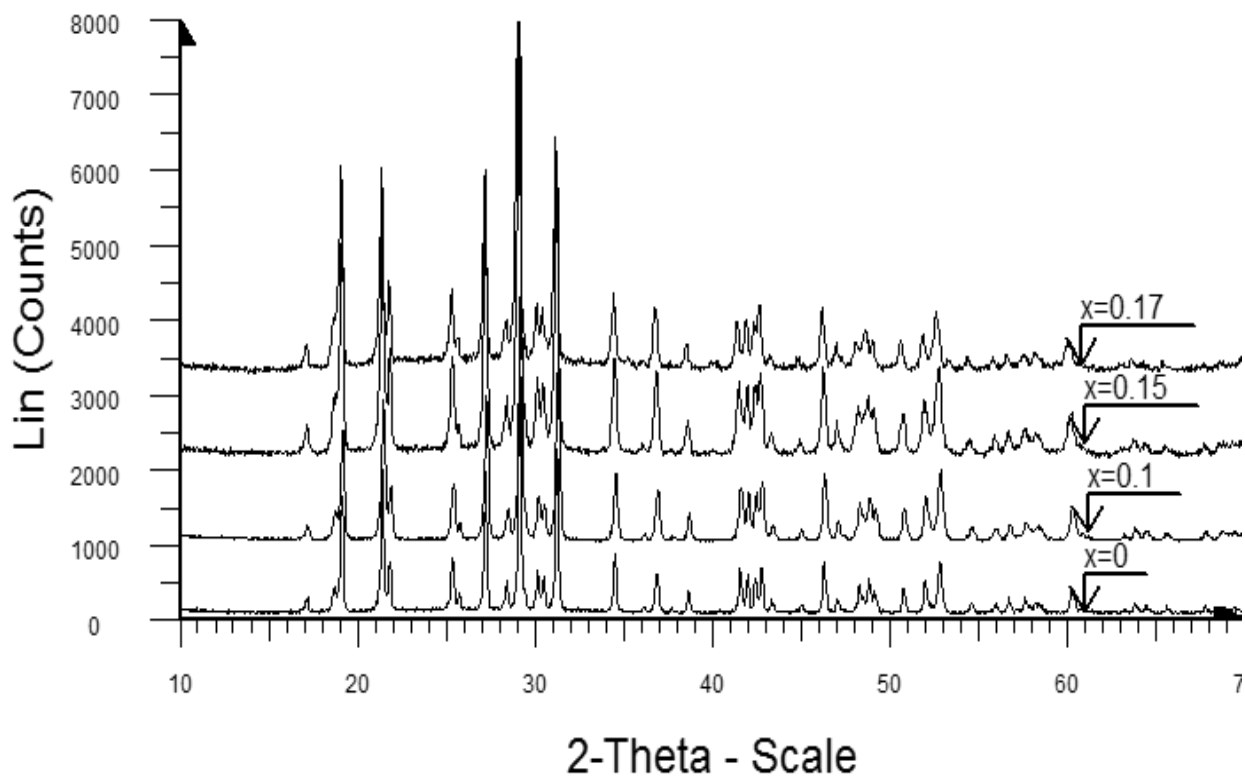


Fig. 2. X-ray diffraction spectra of unsupported $\text{BiP}_{1-x}\text{V}_x\text{O}_4$ catalysts isotype to BiPO_4 [22–26]

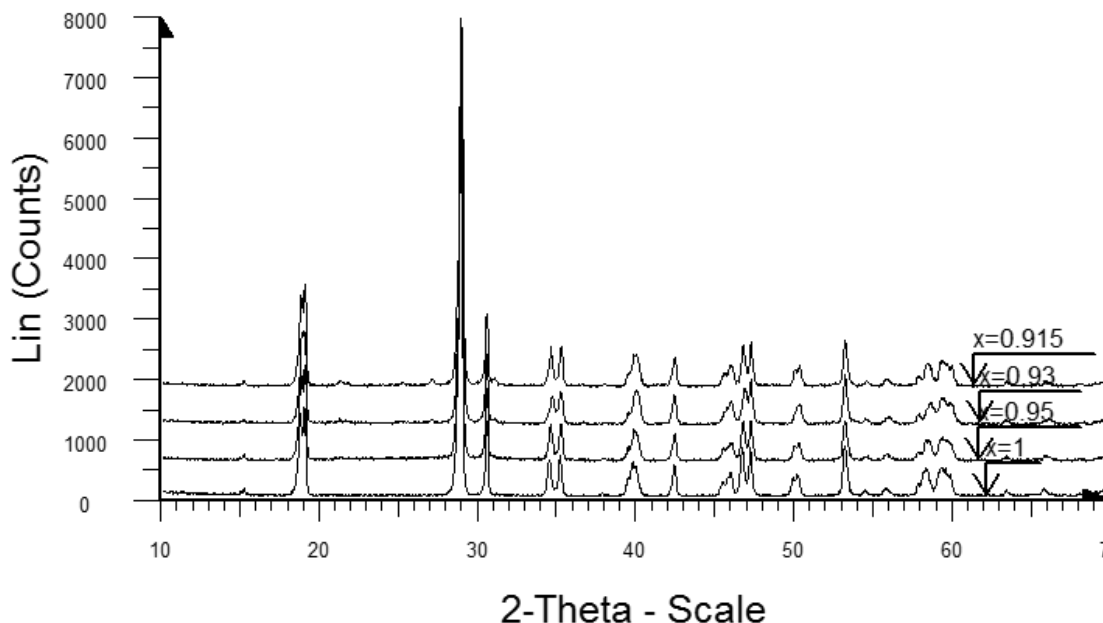


Fig. 3. X-ray diffraction spectra of unsupported $\text{BiP}_{1-x}\text{V}_x\text{O}_4$ catalysts isotype to BiVO_4 [22-26]

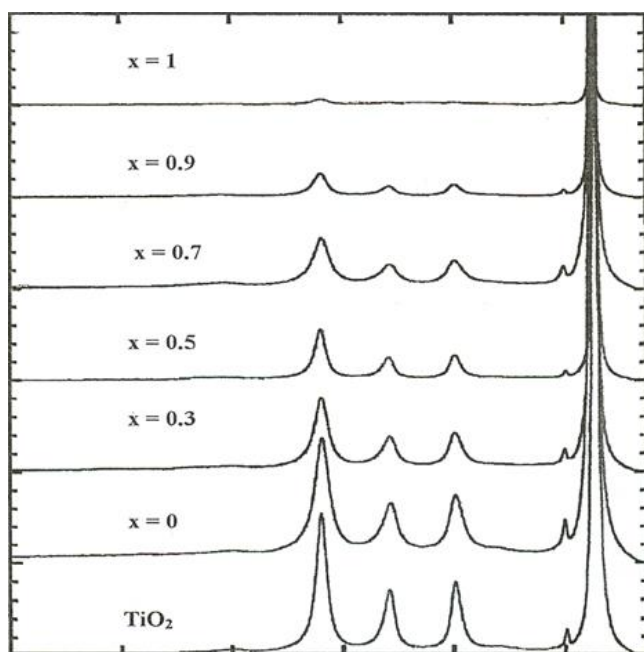


Fig. 4. Raman spectra of $\text{BiP}_{1-x}\text{V}_x\text{O}_4/\text{TiO}_2$ catalysts.

3.1.3. Characterization by TPR

The reducibility of $\text{BiP}_{1-x}\text{V}_x\text{O}_4/\text{TiO}_2$ catalysts was probed by H_2 -TPR, as shown in **Fig. 5**, catalysts with $x < 0.5$ exhibited the same H_2 -TPR characteristic with a double reduction peak at 550°C and 740°C , corresponding successively to the reduction of Bi^{3+} to Bi^{2+} and the reduction of Bi^{2+} to Bi in H_2 [3,28,29].

For solids with $x \geq 0.5$, the TPR profile consists of a broad multi-component peak. In this case, the observed hydrogen consumption corresponds to the reduction of V^{5+} and Bi^{3+} [3,28–30]. The shoulder at a high reduction

temperature (about 630°C for $x = 0.7$ and $x = 1$) may be due to bulk vanadium oxide [30], which is in agreement with XRD results showing that bismuth oxide increases the redox property of the $\text{V}_2\text{O}_5/\text{TiO}_2$ catalyst

An increase in V content shifted the temperature presence of V_3O_7 oxides for these catalysts. Cho et al. obtained the same profile in the $\text{V-Bi-O}/\text{TiO}_2$ catalyst [31,32]. The authors suggest a peak from 560°C for $x = 0.5$ to 630°C for $x = 1$ (as indicated by the dashed line). The H_2 consumption rate (peak area) continuously increases with increasing V content from $x = 0$ to $x = 1$, suggesting lower reducibility of the $\text{BiPO}_4/\text{TiO}_2$ catalyst, this is due to the low dispersion of BiPO_4 species on the titanium support proven by X-ray diffraction. This trend parallels that of the measured propane conversion rates, as shown below. Thus, the initial H_2 reduction steps, rather than the maximum temperatures of the H_2 -TPR curves for the $\text{BiP}_{1-x}\text{V}_x\text{O}_4/\text{TiO}_2$ catalysts, are most relevant to the redox cycles required for propane ODH.

3.1.4. Characterization of acid-base properties

The acid-base properties of various oxides supported on TiO_2 have been investigated by the methanol oxidation test reaction [33,34], which is believed to be structure sensitive. In addition, methanol oxidation is often used as a test reaction to characterize the acid-base properties of catalysts. Thus, the acidic character of a catalyst can be translated by the selectivity towards dimethyl ether and the basic character by the selectivity towards carbon dioxide. The selectivity towards soft oxidation products (methylal) is related to a bi-functional acid-base

Archive of SID

character while the redox character can be related to the formation of formaldehyde obtained by oxidative dehydrogenation [18,34–36].

The catalytic results of methanol oxidation for $\text{BiP}_{1-x}\text{V}_x\text{O}_4/\text{TiO}_2$ are shown in **Table 2**. Formaldehyde is the major product of the reaction for all catalysts except BiPO_4 , which has the highest selectivity for dimethyl ether (DME), indicating the high redox character of all samples. Formaldehyde, which is formed by the Mars-van Krevelen mechanism involving the depletion of surface oxygen atoms [37–39], is the only product representing the number of active redox sites.

The catalytic activity increases globally with the V content and reaches a maximum at $x = 0.3$. This could be due on the one hand to the combination of the elements vanadium, phosphorus, and titanium (V-P-O-Ti), and on the other hand to the reducible properties of this catalyst confirmed by TPR. Compared to the bulk catalysts, the oxides supported by titanium oxide are significantly more active (**Fig. 6**).

On the other hand, the most accurate characterization will be obtained for catalysts with only one type of active site; the dispersion effect due to the different

types of sites could completely mask the variations in catalytic behavior. The possible transformation of the catalyst surface by the reaction and the need for a small number of different active site types are the main limitations of using methanol as a catalyst surface probe. In any case, this indirect surface characterization provides relevant information about the behavior of the catalyst surface, allowing for an effective comparison of a range of supported and unsupported catalysts. Catalyst surface characterization is complementary to other usual characterization techniques (Spectroscopic Raman, X-ray diffraction) and seems to be able to provide the dynamics of the catalyst surface [40].

3.2. Catalytic tests

The catalytic results of $\text{BiP}_{1-x}\text{V}_x\text{O}_4/\text{TiO}_2$ catalysts in the oxidative dehydrogenation of propane are presented in **Table 3**. The main products were propylene, acrolein, ethylene, and CO_2 . The increase in vanadium content leads to better catalytic performance in terms of propylene productivity with better activity (Figure 6), one could think of the presence of large crystallites of V_3O_7 and BiVO_4 species, confirmed by XRD.

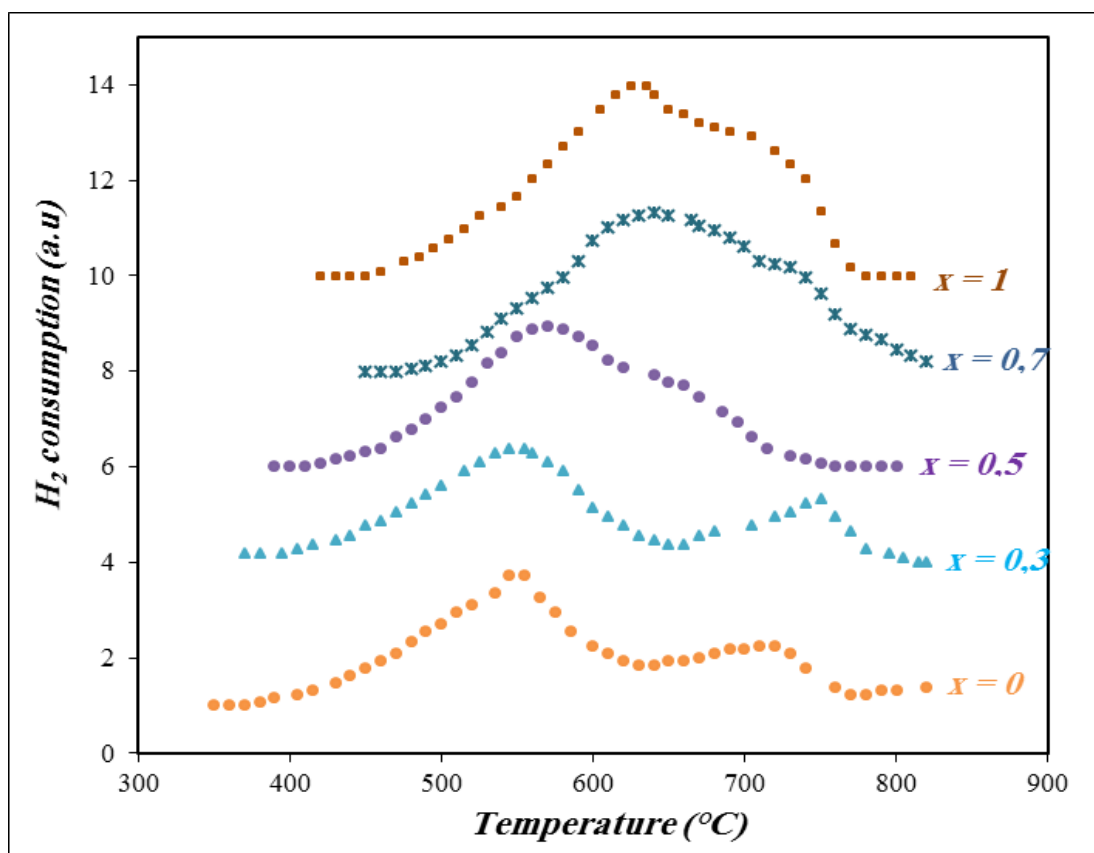
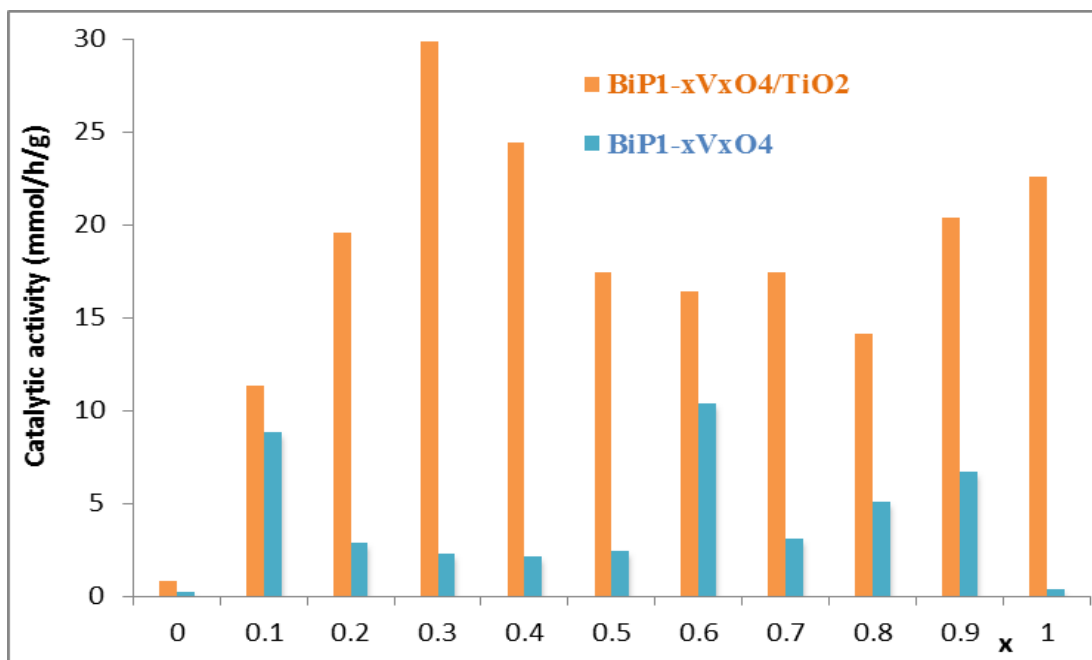


Fig. 5. TPR Profiles of titanium-supported $\text{BiP}_{1-x}\text{V}_x\text{O}_4$ Catalysts. Initial conditions: The temperature was increased from 25 °C to 900 °C at a rate of 5 °C/min.

Table 2. Methanol oxidation on BiP_{1-x}V_xO₄/TiO₂ SamplesReactions conditions: T = 250 °C, CH₃OH/O₂/He = 7.1/15.5/77.4 (mol%)

x	Specific area (m ² /g)	S _{DME} (%)	S _F (%)	S _{FM} (%)	S _M (%)	S _{CO2} (%)	Catalytic activity	
							mmol/h/g	mmol/h/m ²
0	6.3	83.7	8.5	0	6	1.8	0.8	0.13
0.1	5.8	0.9	84.9	3.6	9.3	1.2	11.3	1.95
0.2	6.2	0	89.4	4.4	5.4	0.8	19.6	3.16
0.3	6.6	0	89.3	6.3	3.5	0.9	29.9	4.53
0.4	6.4	0	89.8	5.7	3.3	1.1	24.2	3.78
0.5	6.1	0	90.2	4.6	4.1	1.1	17.4	2.85
0.6	6.0	0	90.0	3	6.3	0.8	16.4	2.73
0.7	6.0	0	90.4	4.2	4.8	0.6	17.4	2.90
0.8	5.9	0	92.2	3.3	3.2	1.2	14.1	2.39
0.9	5.8	0	90.0	4.3	4.9	0.8	20.4	3.52
1	5.6	0	91.5	4.1	3.8	0.6	22.6	4.04

DME: dimethyl ether, F: formaldehyde, FM: methyl mehylformate, M: methylal.

**Fig. 6.** Comparison of the global activity of BiP_{1-x}V_xO₄ and BiP_{1-x}V_xO₄/TiO₂ in methanol oxidation. Reactions conditions: T = 250 °C, CH₃OH/O₂/He = 7.1/15.5/77.4 (mol%).

Moreover, the acid-base nature of the catalyst and support can affect the adsorption/desorption of reactants and products [3,41,42]. This may be the case with our catalysts. The results (Table 3, Fig. 7)) show that when phosphorus is replaced by vanadium, there is an increase in propene activity and selectivity and a sharp decrease in acrolein selectivity. It seems that the formation of acrolein in the presence of BiPO₄/TiO₂ is related to the high acidity of this catalyst, which would prevent the desorption of the propene molecule, thus leading to its oxidation to acrolein.

Allylic oxidation generally occurs at a site with an acidic center and unstable oxygen: the acidic center stabilizes propene by the interaction between the electrons of the double bond and a metal cation, which induces the eventual dislodgement of an H from a CH₃ molecule causing the formation of the allylic intermediate. The dislodgement of a second H and incorporation of oxygen in the formation of acrolein [43, 44]. The substitution of phosphorus by vanadium in TiO₂-supported BiP_{1-x}V_xO₄ catalysts increases the selectivity to olefins during propane ODH. This change in

Archive of SID

selectivity to oxidized hydrogenation products has been correlated with a decrease in the number of acidic sites [45], or a decrease in the heat of adsorption of propylene [46].

In addition, the high propene selectivity of these catalysts may be a consequence of the presence of VO_x species covering the $\text{BiP}_{1-x}\text{V}_x\text{O}_4$ phase formed on the support. These species would be of the type formed during the impregnation of (basic) MgO by vanadium and are selective for propene [41,47,48].

Finally, in **Table 2**, it can be seen that the selectivity towards propene is high for the catalysts containing phosphorus and vanadium, remarkably lower for the catalyst containing only phosphorus ($\text{BiPO}_4/\text{TiO}_2$), and is the highest for the sample containing only vanadium ($\text{BiVO}_4/\text{TiO}_2$).

On the other hand, $\text{BiP}_{1-x}\text{V}_x\text{O}_4/\text{TiO}_2$ catalysts convert propane to propylene, acrolein, and carbon dioxide. The preponderance of these products depends on the structure of the species dispersed on the stitania and the nature of the active sites [38]. It has been proposed in similar work that isolated tetrahedral vanadium species exhibit greater selectivity for propene than octahedral vanadium species (isolated or associated) [49–51]. This may explain why catalysts with x , which have BiVO_4 species on their surface show higher selectivity for propene. In addition to the catalyst structure, the strength of the oxygen bond in the surface VO_x species is a primary parameter that governs the activities and selectivity of titanium-supported vanadium catalysts. In extensive structural studies [49,50], of supported vanadium oxide catalysts, three types of network oxygen bonds have been identified (**Fig. 1**): (a) $\text{V}=\text{O}$ terminal bonds, (b) $\text{V}-\text{O}-\text{V}$ bridging bonds, and (c) $\text{V}-\text{O}-\text{V}$ bridging bonds. Each type of oxygen in the network has different properties. The studies aimed to determine which type of oxygen bond in the network is responsible for the oxidation activity, which occurs in various catalytic oxidation reactions [52]. It was determined that the oxygen of the $\text{V}-\text{O}$ -support bond, rather than the $\text{V}=\text{O}$ or $\text{V}-\text{O}-\text{V}$ terminal bonds, is the one involved in this catalytic oxidation [52].

The increase in activity and selectivity found for the supported catalysts compared to the bulk catalysts (Figure 8) is due to the presence of the TiO_2 support. The latter TiO_2 carries two types of active sites, namely, (reduced sites and Omega sites (stretched siloxane bridges) which are effective in activating O_2 and propane molecules, respectively. Also, the V_3O_7 and BiVO_4 species present on the titanium surface (X-ray

results) generate their own reduced active sites capable of activating oxygen in the gas phase. This statement could explain the ability of $\text{BiP}_{1-x}\text{V}_x\text{O}_4$ supported by titanium to promote the formation and stabilization of its own reduced sites. The effect exerted by $\text{BiP}_{1-x}\text{V}_x\text{O}_4$ on the reactivity of bare TiO_2 and in particular in the oxygen activation process has already been correlated with the density of reduced sites determined RTP- H_2 . Finally, it is concluded that the activity observed with bare TiO_2 is due to some specific surface sites with donor properties to activate molecular oxygen. These sites are positively influenced by the presence of dispersed V_3O_7 and BiVO_4 on the titanium surface for catalysts $x > 0$.

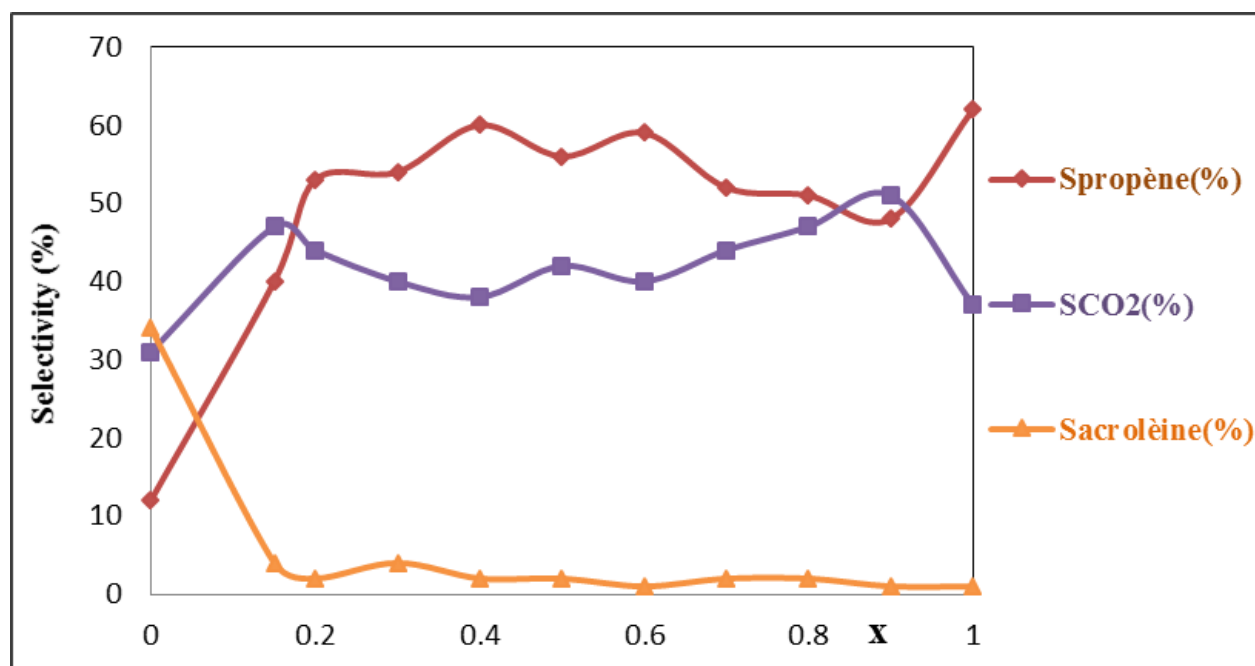
The effect of dispersing the mixed oxides on support is shown in **Fig. 8**, which compares the overall propane ODH activity of the two types of catalysts: bulk and supported. The increase in activity and selectivity seen for the supported catalysts over the bulk catalysts is due to the presence of the TiO_2 support. The latter TiO_2 carries two types of active sites, namely, reduced sites and Omega sites (stretched siloxane bridges) that are effective in activating O_2 and propane molecules, respectively. Furthermore, the V_3O_7 and BiVO_4 species present on the titanium surface (X-ray results) generate their own reduced active sites capable of activating oxygen in the gas phase. This statement could explain the ability of titanium-supported $\text{BiP}_{1-x}\text{V}_x\text{O}_4$ to promote the formation and stabilization of its own reduced sites. The effect exerted by $\text{BiP}_{1-x}\text{V}_x\text{O}_4$ on the reactivity of bare TiO_2 and in particular in the oxygen activation process has already been correlated with the density of reduced sites determined RTP- H_2 . Finally, it is concluded that the activity observed with bare TiO_2 is due to some specific surface sites with donor properties to activate molecular oxygen. These sites are positively influenced by the presence of dispersed V_3O_7 and BiVO_4 on the titanium surface for catalysts $x \geq 0$.

Finally, in **Table 2**, it can be seen that the selectivity to propene is high for the phosphorus and vanadium-containing catalysts, remarkably lower for the phosphorus-only catalyst ($\text{BiPO}_4/\text{TiO}_2$) and is the highest for the sample with only vanadium ($\text{BiVO}_4/\text{TiO}_2$).

Fig. 9, illustrates the evolution of the selectivity for propene as a function of the conversion of $\text{BiP}_{0.7}\text{V}_{0.3}\text{O}_4/\text{TiO}_2$ and $\text{BiP}_{0.4}\text{V}_{0.6}\text{O}_4/\text{TiO}_2$ catalysts, when the conversion increases the propene selectivity decreases. This would indicate good dispersion of these oxides on TiO_2 support.

Table 3. Product distribution in ODH of Propane over BiP_{1-x}V_xO₄/TiO₂ catalysts.Reactions conditions: T = 480 °C, C₃H₈/O₂/He = 10/10/80 (mol%).

x	Conv (%)	S _{propene} (%)	S _{CO₂} (%)	S _{acroleine} (%)	S _{ethylene} (%)	Catalytic activity	
						mmol/h/g	mmol/h/m ²
0	14	12	31	34	0	1.04	0.17
0.1	20	40	47	4	2	1.5	0.26
0.3	24	54	40	4	2	1.79	0.27
0.4	18	60	38	2	0	1.36	0.21
0.5	19	56	42	2	0	1.46	0.24
0.6	17	59	40	1	0	1.25	0.21
0.7	19	52	44	2	3	1.46	0.24
0.8	17	51	47	2	0	1.26	0.21
0.9	18	48	51	1	1	1.36	0.235
1	17	62	37	1	0	1.33	0.24

**Fig. 7.** Evolution of the Selectivity to propylene propelene, acrolein, and CO₂ with different vanadium Concentrations in the propane ODH. Reactions conditions: T = 480 °C, C₃H₈/O₂/He = 10/10/80 (mol%).

When the rates of the reaction products are considered, a good correlation can be done between the formaldehyde and the propene rates of formation (**Fig. 10**), strongly suggesting that these reactions occur on the same surface sites and consequently require the same strong redox catalytic properties.

The catalytic of titanium-supported BiP_{1-x}V_xO₄ catalysts can be related to their redox properties. It has been postulated that the catalytic activity and selectivity of an oxide in selective oxidation can be related to the

reduction rate of the oxide. Over an oxide which is very difficult to reduce, the activity will be low. An active and selective catalyst should have intermediate ease of reduction [49,52]. The comparison between the propene activity and the temperature of the main TPR peaks corresponding to the reduction of V⁵⁺ (**Fig. 11**) leads to a good correlation between these two parameters. The reduction peak of the BiP_{0.7}V_{0.3}O₄/TiO₂ catalyst was lower than that of the other catalysts, indicating that in this case, the easier the reduction of the catalyst, the greater its activity.

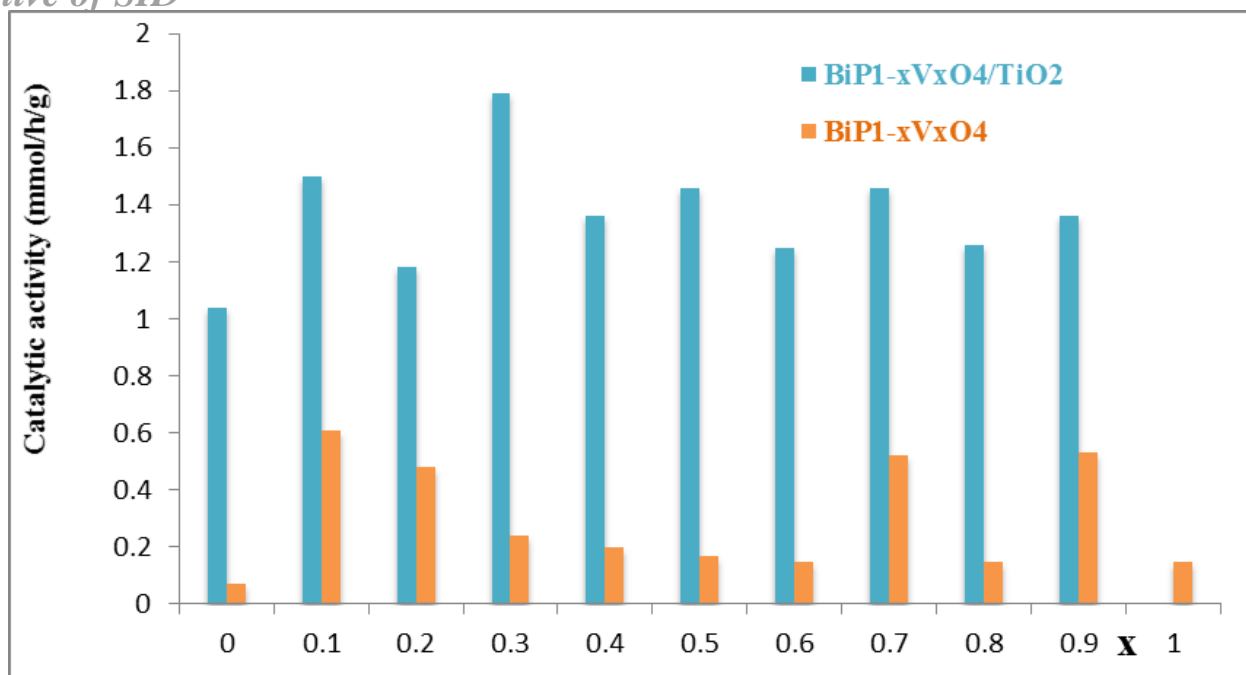


Fig. 8. The comparison of the global activity of BiP_{1-x}V_xO₄ and BiP_{1-x}V_xO₄/TiO₂ in the ODH of propane reaction. Reactions conditions: T = 480 °C, C₃H₈/O₂/He = 10/10/80 (mol%).

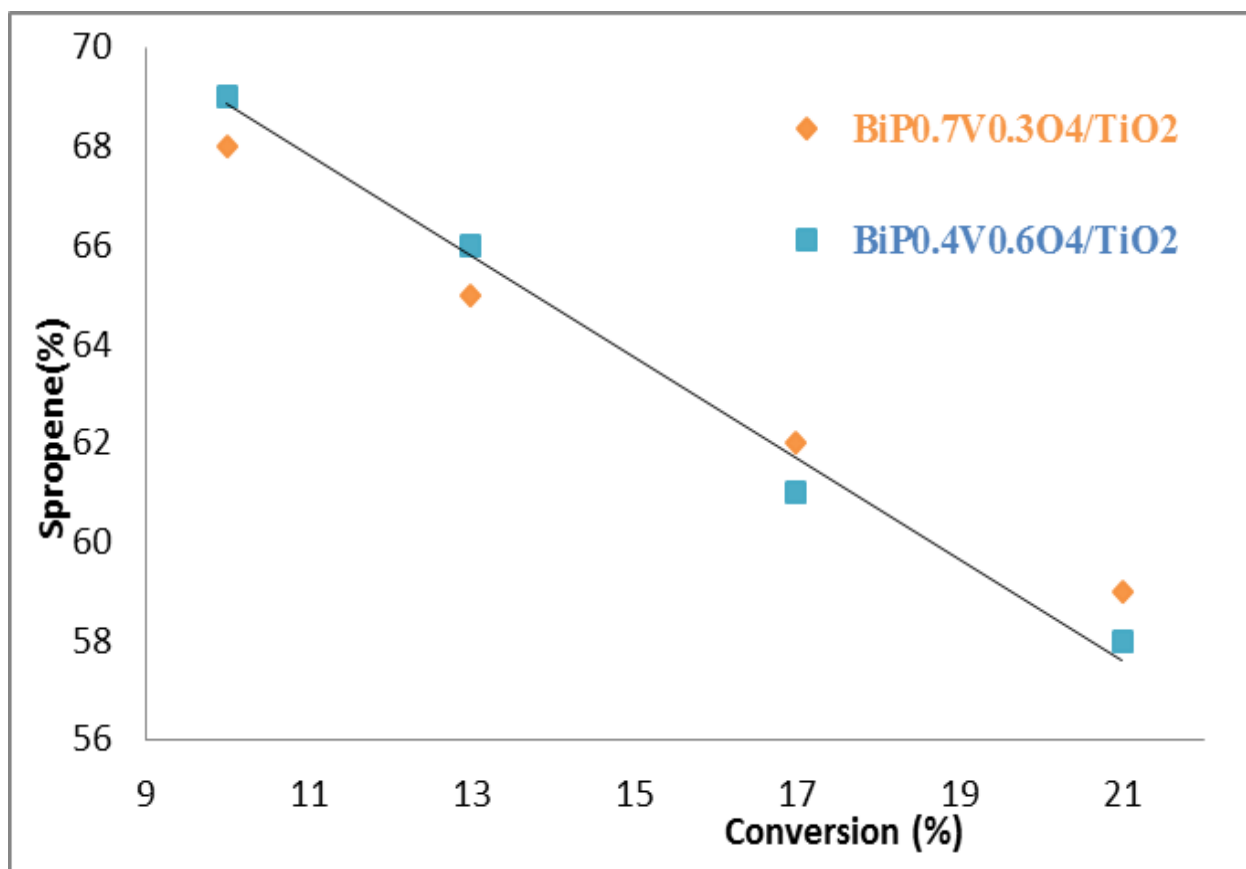


Fig. 9. Evolution of the selectivity for propene as a function of the conversion for Catalysts BiP_{0.7}V_{0.3}O₄/TiO₂ and BiP_{0.4}V_{0.6}O₄/TiO₂. Reactions conditions: T = 480 °C, C₃H₈/O₂/He = 10/10/80 (mol%).

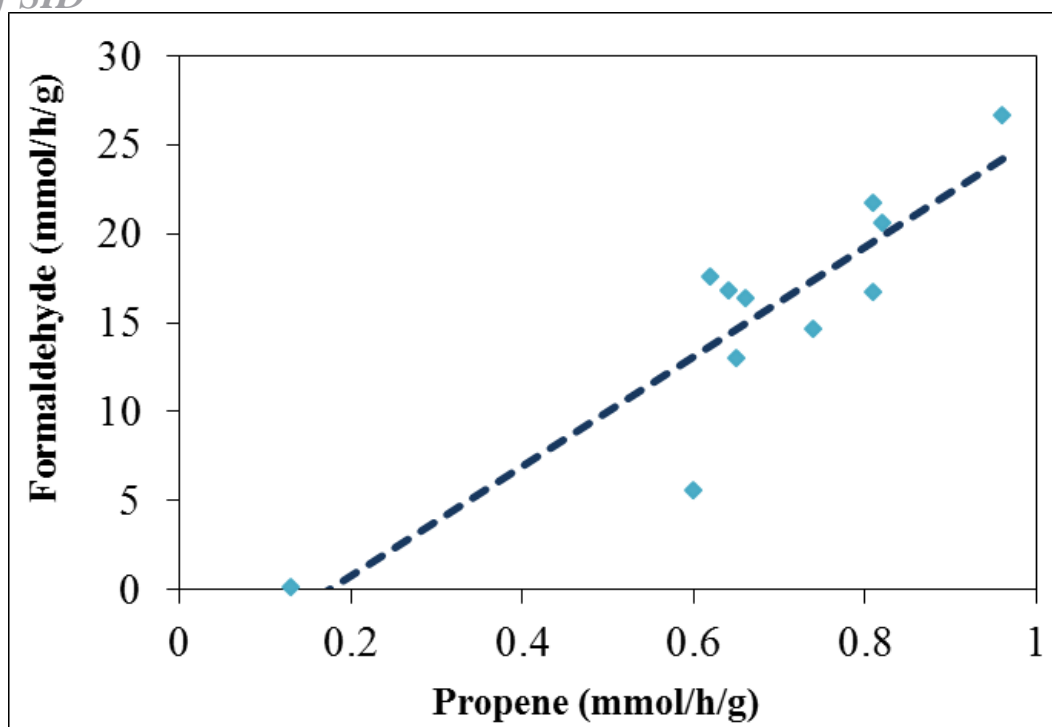


Fig. 10. Correlation between the formation rates of formaldehyde and propene.

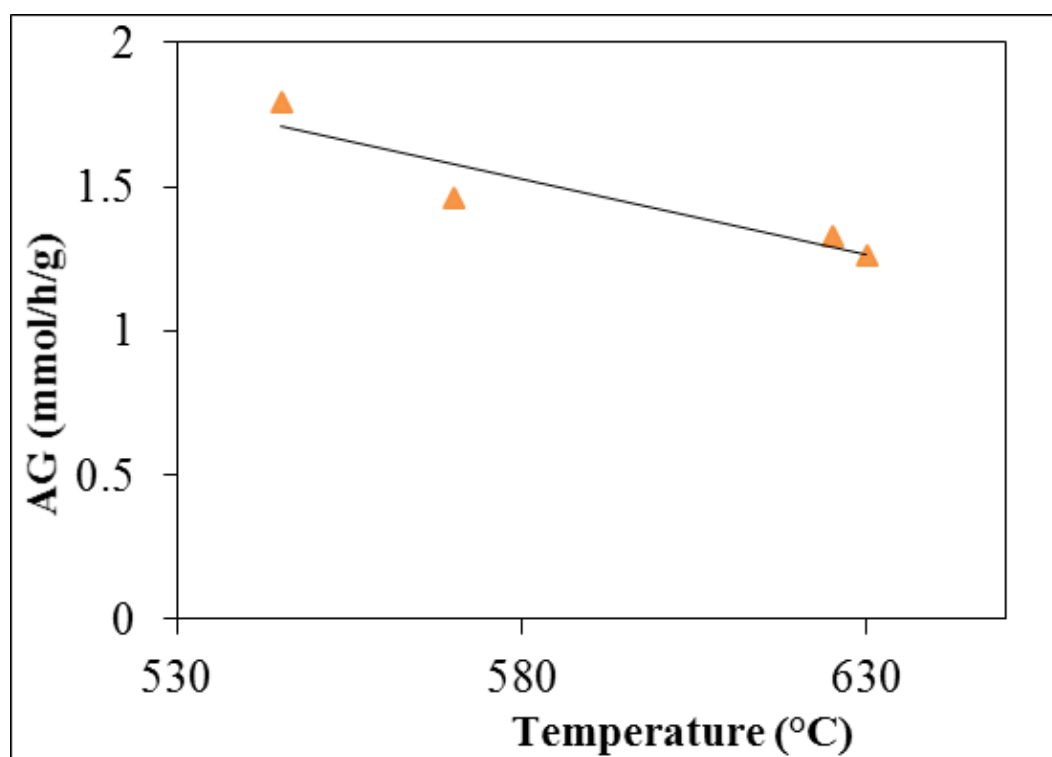


Fig. 11: Correlation of the position of the TPR peaks between 500 °C and 650 °C of $\text{BiP}_{1-x}\text{V}_x\text{O}_4/\text{TiO}_2$ with the selectivity and formation rate of propene.

4. Conclusions

The activities and selectivity's of the propane ODH reaction depend significantly on the structures of the BiPO_4 and BiVO_4 species present on the titanium

support and also depend strongly on the redox properties determined by the methanol test reaction and TPR measurements. With increasing V content, the structures present on the support evolve from BiPO_4 to isolated crystallites of BiVO_4 and V_3O_7 . The isolated BiVO_4 are

Archive of SID

more active due to their higher reducibility, whereas BiPO₄ crystallites are significantly less selective for propylene in propane ODH. This superiority of BiVO₄ crystallites in propylene formation is consistent with their reducible properties, and the presence of redox sites confirmed by methanol oxidation. This reaction is a very sensitive method for detecting very small changes in the nature of the catalytically active phase of BiP_{1-x}V_xO₄/TiO₂ catalysts. Any structural modification of the catalytic site generally leads to an observable evolution of the selectivity. This study provides fundamental information useful for the design and construction of supported BiP_{1-x}V_xO₄ catalysts with desirable crystal structures for the efficient production of propylene and acrolein from propane ODH. These new results provide fundamental information on the molecular structure-redox site-reactivity/selectivity relationships of molecularly dispersed TiO₂-supported oxides. Compared to unsupported BiP_{1-x}V_xO₄, impregnation of this oxide on TiO₂ increases the accessible surface area and promotes propene formation. The latter may result from an increase in redox character with increasing vanadium content. The reducibility of these solids is more important, thus inducing an increase in of the activity. The Physico-chemical studies carried out on these solids did not allow to clearly define defining the nature of the interaction between the support and the active phase of these catalysts. We can only conclude that the bismuth-vanadium-phosphorus-TiO₂ mixture leads to an improvement in of the catalytic performances.

Acknowledgements

Great tribute to Jean Michel Tatibouët research director in Joël Barrault's team at LACCO in Poitiers, who supported and directed my internship at LACCO. I would like to dedicate this article to his memory.

References

- [1] H.H. KUNG, Adv. Catal. 40 (1994) 1–38.
- [2] E.A. Mamedov, V. Cortés Corberán, Appl. Catal. A, Gen. 127 (1995) 1–40.
- [3] J.M.L.N. T. Blasco, Appl. Catal. A Gen. 157 (1997) 117–142.
- [4] R. Grabowski, Catal. Rev. Sci. Eng. 48 (2007) 199–268.
- [5] F. Cavani, N. Ballarini, A. Cericola, Catal. Today 127 (2007) 113–131.
- [6] J.J.H.B. Sattler, J. Ruiz-Martinez, E. Santillan-Jimenez, B.M. Weckhuysen, Chem. Rev. 114 (2014) 10613–10653.
- [7] W. Zhu, X. Chen, J. Jin, X. Di, C. Liang, Z. Liu, Chinese J. Catal. 41 (2020) 679–690.
- [8] M. OUCHABI, I. LOULIDI, M. AGUNAOU, Iran. J. Chem. Chem. Eng. (2022).
- [9] L. Savary, J. Saussey, G. Costentin, M.M. Bettahar, M. Gubelmann-Bonneau, J.C. Lavalley, Catal. Today 32 (1996) 57–61.
- [10] P. Nagaraju, N. Lingaiah, P.S.S. Prasad, V.N. Kalevaru, A. Martin, Catal. Commun. J. 9 (2008) 2449–2454.
- [11] and T.M. N. Ballarina, F. Cavana*, C. Cortellia, S. Ligia, F. Pierellia, F. Trifiro` a, C. Fumagallib, G. Mazzonib, Top. Catal. 38 (2006) 147–156.
- [12] S. Arias-pe, R. Garcı, B.E. Handy, S. Robles-andrade, G. Sandoval-robles, V. Di, Ind. Eng. Chem. Res. 48 (2009) 1215–1219.
- [13] B.G. A. Klisin´ska, K. Samson, I. Gressel, Appl. Catal. A Gen. 309 (2006) 10–16.
- [14] A. Caldarelli, F. Cavani, F. Folco, S. Luciani, C. Cortelli, R. Leanza, in: Catal. Today, 2010, pp. 204–210.
- [15] M. Ruitenbeek, A.J. Van Dillen, A. Barbon, E.E. Van Faassen, D.C. Koningsberger, J.W. Geus, Catal. Letters 55 (1998) 133–139.
- [16] M.P. Casaletto, G. Landi, L. Lisi, P. Patrono, F. Pinzari, "Journal Mol. Catal. A, Chem. 329 (2010) 50–56.
- [17] C.A. Carrero, R. Schloegl, I.E. Wachs, R. Schomaecker, ACS Catal. 4 (2014) 3357–3380.
- [18] B. Solsona, A. Dejoz, M.I. Vázquez, F. Márquez, J.M. López Nieto, Appl. Catal. A Gen. 208 (2001) 99–110.
- [19] H. Zhang, S. Cao, Y. Zou, Y. Wang, X. Zhou, Y. Shen, X. Zheng, Catal. Commun. 45 (2014) 158–161.
- [20] S.J.K. Miguel A. Ban~ares*, Catal. Today 96 (2004) 251–257.
- [21] A.A. Lemonidou, L. Nalbandian, I.A. Vasalos, Catal. Today 61 (2000) 333–341.
- [22] R.A. Overbeek, P.A. Warringa, L.M. Visser, A.J. Van Dillen, J.W. Geus, Appl. Catal. A Gen. 135 (1996) 209–230.
- [23] J.M. Tatibouët, Appl. Catal. A Gen. 148 (1997) 213–252.

Archive of SID

- [24] AGUNAOU M., OUCHABI M., Ann. Chim. Sci. Des Matériaux 25 (2000) 17–20.
- [25] C. Ding, A. Han, M. Ye, Y. Zhang, L. Yao, J. Yang, RSC Adv. 8 (2018) 19690–19700.
- [26] X. Li, F. Li, X. Lu, S. Zuo, Z. Li, C. Yao, C. Ni, Powder Technol. 327 (2018) 467–475.
- [27] R. Luschtinetz, J. Frenzel, T. Milek, G. Seifert, J. Phys. Chem. C 113 (2009) 5730–5740.
- [28] H.-I.L. Sang-Gi Lee, Korean J. Chem. Eng. 15 (1998) 463–468.
- [29] B.R. Jermy, B.P. Ajayi, B.A. Abussaud, S. Asaoka, J. OfMolecular Catal. A Chem. (2015).
- [30] Y. Cho, D. Park, D. Park, Res. Chem. Intermed. 28 (2002) 419–431.
- [31] Y. Cho, B. Hwang, D. Park, H. Woo, J. Chung, Korean J. Chem. Eng. 19 (2002) 611–616.
- [32] Y.G. Cho, H.C. Woo, J.S. Chung, Res. Chem. Intermed. 2002 285 28 (2002) 419–431.
- [33] A.S. Elmi, E. Tronconi, C. Cristiani, J.P.G. Martin, P. Forzatti, G. Busca, Ind. Eng. Chem. Res. 1989, 28 (1989) 387–393.
- [34] I.E.W. Goutam Deo, J. Catal. 146 (1994) 323–334.
- [35] J.M. Parera, X.S. Figoli, J. Catal. 14 (1969) 303–310.
- [36] J.M. Tatibouet, Appl. Catal. A Gen. 148 (1997) 213–252.
- [37] R. Grabowski, B. Grzybowska, A. Kozłowska, J. Słoczyński, K. Wcisło, Y. Barboux, Top. Catal. 3 (1996) 277–288.
- [38] P. Concepción, J.M.L. Nieto, J. Pérez-Pariente, J. Mol. Catal. A Chem. 97 (1995) 173–182.
- [39] M. Nehate, V. V. Bokade, Appl. Clay Sci. 44 (2009) 255–258.
- [40] C. Ding, A. Han, M. Ye, Y. Zhang, L. Yao, J. Yang, RSC Adv. 8 (2018) 19690–19700.
- [41] P. Concepcion, J.M.L. Nieto, J. Mol. Catal. A Chem. 99 (1995) 173–182.
- [42] R. Grabowski, B. Grzybowska, A. Kozłowska, J. Stoczyński, K. Wcisło, Top. Catal. 3 (1996) 277–288.
- [43] J.D.B. ROBERT K. GRASSELLI, Adv. Catal. 30 (1981) 133–162.
- [44] O.S. M. Baems, O.V. Buyevskaya, M. Kubik, G. Maiti, O. Ovsitser, Catal. Today 33 (1997) 85–96.
- [45] R. Grabowski, B. Grzybowska, K. Samson, J. Stoczyński, J. Stoch, K. Wcisło, Appl. Catal. A Gen. 125 (1995) 129–144.
- [46] j. p. B. Dominique Courcot, Anne Ponchel, Barbara Grzybowska, Yolande Barboux, Monique Rigole, Michel Guelton, Catal. Today 33 (1997) 109–118.
- [47] J.M.L.N. P. Concepcion, A. Galli, Top. Catal. 3 (1996) 451–460.
- [48] F. Arena, F. Frusteri, A. Parmaliana, Catal. Letters 60 (1999) 59–63.
- [49] S. Zhang, H. Liu, Appl. Catal. A Gen. 573 (2019) 41–48.
- [50] F. Arena, F. Frusteri, A. Parmaliana, Catal. Lett. 1999 601 60 (1999) 59–63.
- [51] P. Concepción, A. Galli, J.M. López Nieto, A. Dejoz, M.I. Vazquez, Top. Catal. 1996 33 3 (1996) 451–460.
- [52] H. Nair, C.D. Baertsch, J. Catal. 258 (2008) 1–4.